

# Relativistic calculation of dielectronic recombination on the $C^{4+}$ ground state

Yu Zou,<sup>1,2</sup> Yue-Ming Li,<sup>1</sup> Yong Liu,<sup>1</sup> and Quan-Yu Fang<sup>1</sup>

<sup>1</sup>*Institute of Applied Physics and Computational Mathematics, P.O. Box 8009, Beijing 100088, People's Republic of China*

<sup>2</sup>*Center of Atomic and Molecular Science, Tsinghua University, Beijing 100083, People's Republic of China*

(Received 21 October 2000; published 12 April 2001)

The measurement of the dielectronic recombination (DR) cross section of  $C^{4+}$  with a high resolution [S. Mannervik *et al.*, Phys. Rev. A **55**, 1810 (1997)] provides a rigorous test case for various theoretical methods. In the earlier work, the relativistic multichannel theory was applied to the DR process on the  $He^+$  ion for both the  $\Delta N=1$  and  $\Delta N=2$  transitions with a principal quantum number of the outermost electron up to 5. In principle, that method can be applied to resonances with any high principal quantum numbers. Practically, however, the calculations become very time consuming. In the present work, the method is extended by incorporating the Bell-Seaton theory. The DR cross sections of  $C^{4+}$  for the resonances with  $2 \leq n \leq 25$  are calculated. The results are in good agreement with those of the experiment except for the  $n=6$  and 7 resonances. According to the present calculation, the Rydberg cutoff due to field ionization could be about  $n_{\max}=25$  instead of  $n_{\max}=16$  to take into account the effect of the radiative decay during the time of flight. A sudden decrease is observed between the  $n=7$  and 8 resonances due to the opening of the  $1s2s^1S\epsilon l$  continuum. From the agreement with experiment, it would appear that the present method is applicable to both the low- $n$  and high- $n$  resonances.

DOI: 10.1103/PhysRevA.63.052703

PACS number(s): 34.80.Kw, 32.90.+a, 32.80.Hd

## I. INTRODUCTION

Dielectronic recombination (DR), which composes the resonant component of radiative recombination (RR), is practically important and fundamentally interesting [1–5]. In astrophysical and laboratory plasmas, DR affects the ionization balance and also causes energy losses since the charge state of the ion changes and a photon is emitted in the process. Fundamentally, the studies of DR are significant not only for their provision of a better understanding of the correlations in the doubly excited states but also because of their revelation of the relativistic effect [6] and radiation damping [7–10]. After the experimental observation of Kilgus *et al.* [11], Mannervik *et al.* [12] remeasured the DR cross section of  $C^{4+}$  for the  $\Delta N=1$  transitions with a much higher energy resolution. More resonances with  $n \leq 3$  were resolved and the peaks for  $n=6,7$  were fully separated. This measurement provides a more rigorous test case for various theoretical methods.

In the earlier work [13], the relativistic multichannel theory (RMCT) [14–16] was applied to the DR process on the  $He^+$  ion for both the  $\Delta N=1$  and  $\Delta N=2$  transitions with the principal quantum number of the outermost electron up to 5. A good agreement with the experiment [17,18] was achieved for the  $n \leq 3$  resonances and the effect of field ionization for the higher- $n$  resonances was elucidated. In principle, that method can be applied to the resonances with any high principal quantum numbers. But practically the calculations become very time consuming because the resonances tend to be narrower and more partial waves have to be taken into account. In the present work, the DR cross sections of  $C^{4+}$  for the  $n \leq 4$  resonances are calculated with the RMCT method. For the resonances with  $4 \leq n \leq 25$ , the Bell-Seaton (BS) theory [19] is incorporated with the RMCT to obtain the cross sections for 12 partial waves. The whole experimental spectrum is reproduced by convolving the cross sec-

tions with the pseudo-Maxwellian distribution [20] of electrons. The results are in good agreement with those of the observation [12] except for the  $n=6$  and 7 resonances where the theory overestimates the intensities by about 15% at the peaks. This discrepancy may be attributed to the couplings between the closed channels or to the effect of field ionization. According to the present calculation, the Rydberg cutoff due to field ionization could be about  $n_{\max}=25$  instead of  $n_{\max}=16$ , taking into account the effect of the radiative decay during the time of flight. A sudden decrease is observed between the  $n=7$  and 8 resonances due to the opening of  $1s2s^1S\epsilon l$  continuum. A dim resonance is identified that may be derived from the  $1s2p^2P$  state through the spin-orbit interaction.

## II. THEORETICAL METHOD

According to the general DR theory of Davies, Bell, and Seaton [7,19], the DR probability for a given incident channel  $j$  can be expressed as  $P_j^{DR} = \sum_{\beta\mu} |S_{\beta\mu,j}|^2$ , with

$$S_{\beta\mu,j} = -2\pi i \sum_{\beta'\mu'} (1+L)_{\beta\mu,\beta'\mu'}^{-1} D_{j,\beta'\mu'},$$

where  $D_{j,\beta\mu}(E) = \langle \Psi_{jE} | P^{(\mu)} | \Psi_{\beta} \rangle$  is the radiative transition matrix element, and the matrix  $L$  represents the high-order effect of radiation. It is explained physically as the radiation damping effect.  $\Psi_{jE}$  and  $\Psi_{\beta}$  are wave functions of the initial continuum states and the final bound states, respectively, and  $P^{(\mu)}$  is the dipole operator of radiative transitions with photo polarization  $\mu$ .

In the present work  $\Psi_{jE}$  is computed with RMCT and  $\Psi_{\beta}$  is obtained by using the configuration-interaction method. The wave function of the continuum state for a specific incident wave  $\varphi_{iE}$  can be expanded as [21]

$$\Psi_{iE} = \sum_n \frac{K_{n,iE} N_{iE}}{E - E_n^{(0)}} \varphi_n + \sum_{i'} P \int_{\epsilon_c} \frac{K_{i'\epsilon,iE} N_{iE}}{E - \epsilon} \varphi_{i'\epsilon} d\epsilon + \varphi_{iE} N_{iE}, \quad (1)$$

where  $\varphi$  is the basic vector and  $P$  indicates the principal integral. The matrix  $K$  can be obtained by solving the Lippman-Schwinger-type equations [14,16], and  $N_{iE} = [1 + \pi^2 \sum_j K_{ji}^2(E)]^{-1/2}$  is the normalization factor, where  $K_{ji}(E) = K_{jE,iE}$  is the on-the-energy-shell element of  $K_{jE',iE}$ . The first and second terms in Eq. (1), respectively, represent the resonance component and the scattering waves for the specific incident wave  $\varphi_{iE}$ . Only the first term is retained in the calculation of the transition matrix elements for the DR process. In the calculation of the  $K$  matrix, the lower limit  $\epsilon_c$  of the integral for each channel in Eq. (1) takes the value of the middle energy between the states with the principal quantum numbers of 9 and 10. Besides discrete states, the infinitely high Rydberg states with the principal quantum numbers larger than 9 and the conjunctive continuum states are also included in the integral as channels. All required bound and continuum orbitals are generated using a Dirac-Fock-Slater potential that is obtained by the self-consistent iteration procedure in the configuration of  $1s^2 8k$ . To resolve the doubly excited states in each symmetry of total angular momentum and parity  $J^\pi$ , the corresponding energy region is scanned. The effective principal quantum number  $\nu$  of the first closed channel is adopted to control the energy step that is automatically adjustable below a maximum step of 0.001 to ensure the full resolution of the important resonances.

Considering the radiation rates are much smaller than the Auger rates for low- $n$  resonances of light ions, the first order of  $S_{\beta\mu,j}$  with  $S_{\beta\mu,j} = -2\pi i D_{j,\beta\mu}$  is adopted for the  $n \leq 4$  resonances. However, the neglect of the radiation width would lead to a nontrivial probability overestimation for the very narrow resonances with a radiation width comparable to the Auger width. A correction has been adopted to those very narrow resonances to include the radiation width. Assuming the isolate-resonance approximation is valid for such narrow resonances, the corrected DR probability  $\bar{P}^{DR}(E)$  is expressed as

$$\bar{P}^{DR}(E) = \frac{AR}{(E - E_0)^2 + \frac{1}{4}(A + R)^2}.$$

The Auger rate  $A$ , the radiative rate  $R$ , and the position  $E_0$  can be obtained by fitting the original DR probability to

$$P^{DR}(E) = \frac{AR}{(E - E_0)^2 + \frac{1}{4}A^2}$$

in the vicinity of each resonance.

For the numerous resonances with  $n \geq 5$ , the direct calculation with the RMCT is infeasible. In this case, the multi-channel quantum defect theory (MQDT) of the DR process

[19] is incorporated with the RMCT to obtain the DR probability. According to BS theory, the DR probability can be expressed as

$$P_j = 1 - \sum_i |S_{ji}|^2$$

with

$$S_{oo} = \chi_{oo} - \chi_{oc} [\chi_{cc} - g \exp(-2\pi i \nu)]^{-1} \chi_{co} \quad (2)$$

and

$$g = \exp(\pi \nu^3 R / z^2).$$

The radiative transition probability  $R$  represents the decay rate of ion core. Equation (2) is valid for the high- $n$  resonances where the transition probably of the outer electron is negligible. The unphysical scattering matrix  $\chi$  can be written as

$$\chi_{ji} = \sum_\alpha U_{j\alpha} \exp(2i\pi \mu_\alpha) U_{i\alpha}. \quad (3)$$

The MQDT physical parameters [22] (the eigenchannel quantum defect  $\mu_\alpha$  and the transformation matrix  $U_{i\alpha}$ ) are obtained with the RMCT from the first principle. These parameters vary slowly and smoothly with respect to the energy in the vicinity of each threshold. Therefore, it is unnecessary to solve the Lippman-Schwinger-type equations point by point in the high- $n$  region. In the present work, only five energy points are computed in the vicinity of threshold and then an interpolation or extrapolation is performed to obtain the parameters at any energy in the high- $n$  region. Since Eq. (2) can describe only one specific transition of ion core, the calculated  $\chi$  matrix is partitioned according to the state of ion core before incorporation with the BS theory. This partition partially neglects the coupling effect of closed channels that belongs to the different ionization threshold. But this coupling effect is included in the elements of matrix  $\chi$ .

### III. RESULTS AND DISCUSSION

The partial cross sections calculated by the RMCT method are shown in Fig. 1 for the  $n \leq 4$  resonance states. Since the effective quantum number of the horizontal axis corresponds to the first closed channel, namely  $1s2s^3S\nu l$ , the resonances of  $n=4$  converging to higher ionization limits ( $1s2s^1S$  or  $1s2p^3P$ ) extend to  $\nu=4.6$ . It can be observed that the partial cross sections exhibit the same features for the total angular momentum and parity  $J^\pi = \frac{3}{2}^+$  and  $\frac{5}{2}^+$ . This similarity can also be found for other pairs of  $(\frac{7}{2}^+, \frac{9}{2}^+)$ ,  $(\frac{1}{2}^-, \frac{3}{2}^-)$ , and  $(\frac{5}{2}^-, \frac{7}{2}^-)$ . The similarity is determined by the incident channel. For  $J^\pi = \frac{3}{2}^+$  and  $\frac{5}{2}^+$  the incident channels are  $1s^2 \epsilon d_{3/2}$  and  $1s^2 \epsilon d_{5/2}$ , respectively. For the low  $Z$  ion of  $C^{3+}$  the spin-orbit interaction is very weak and the  $LS$  coupling is valid. Both incident channels belong to the same  $LS$  symmetry of  ${}^2D^e$ . The resonance states for  $J^\pi = \frac{3}{2}^+$  and  $\frac{5}{2}^+$  must belong to this symmetry too. The cross sections for  $J^\pi = \frac{3}{2}^+$  and  $\frac{5}{2}^+$  exhibit the feature of  ${}^2D^e$  sym-

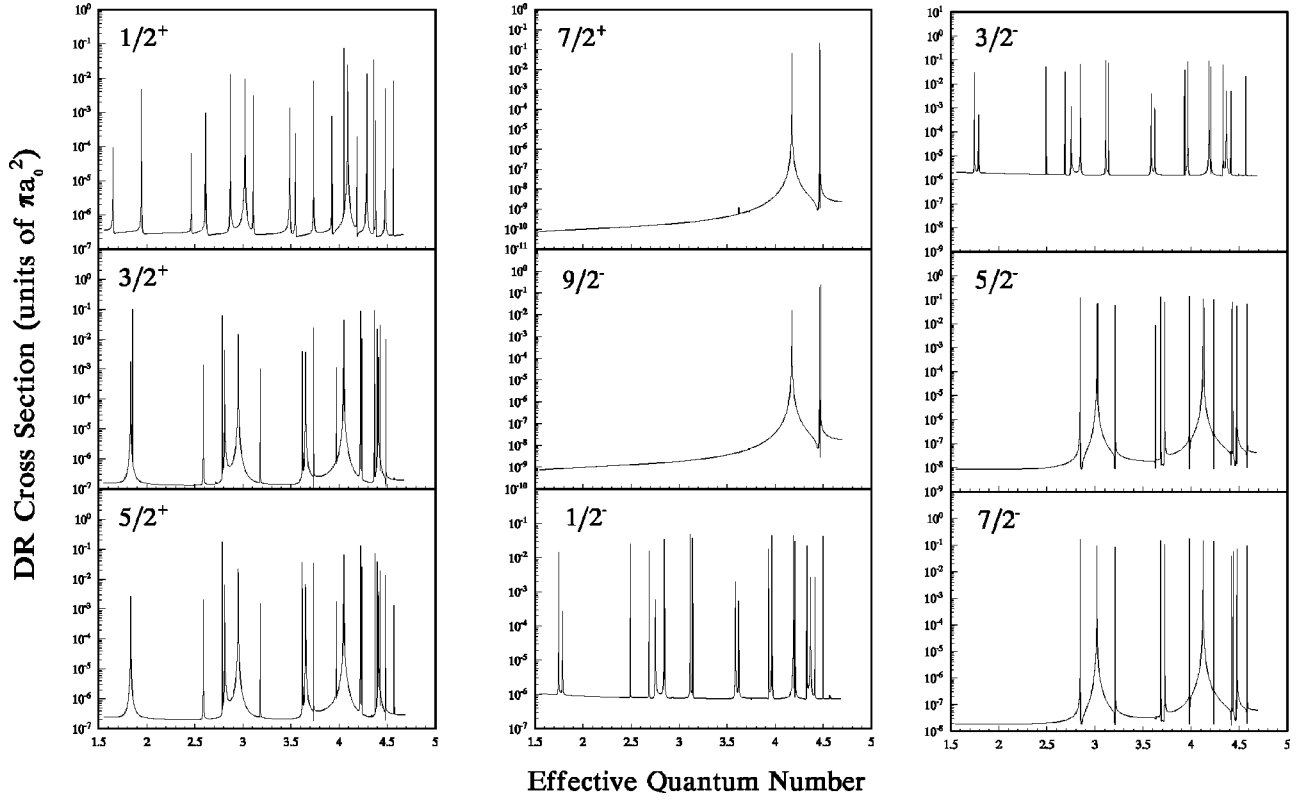


FIG. 1. Partial cross sections calculated with the RMCT method vary with respect to the effective quantum number for the  $n \leq 4$  resonance states.

metry. The  $(\frac{7}{2}^+, \frac{9}{2}^+)$ ,  $(\frac{1}{2}^-, \frac{3}{2}^-)$ , and  $(\frac{5}{2}^-, \frac{7}{2}^-)$  partial waves correspond to the  $LS$  symmetry of  ${}^2G^e$ ,  ${}^2P^o$ ,  ${}^2F^o$ , respectively. The  $\frac{1}{2}^+$  partial wave corresponds to  ${}^2S^e$  symmetry.

In order to compare with experimental measurement, the calculated DR cross sections are convolved with the electron distribution of the pseudo-Maxwellian [20]. Figure 2 shows the convolved partial cross sections. The vertical temperatures  $T_{\perp}$  and longitudinal temperatures  $T_{\parallel}$  are 80 (120) meV and 0.11 (1.5) meV for the solid (dotted) lines, respectively. The two pairs of temperatures are obtained by fitting to the experimental spectra of Mannervik *et al.* [12] and Kilgus *et al.* [11]. By comparing the partial cross sections in the same  $LS$  symmetry, one can find that the ratio of the maximum of each peak is approximately equal to the ratio of the statistical weight of the final state in the DR process, namely,  $(2J+1)/(2J'+1)$ . That indicates the total orbital angular momentum and spin of  $LS$  are good quantum numbers for these resonances. However, an exception can be found in the  $J^{\pi} = \frac{3}{2}^+$  and  $\frac{5}{2}^+$  waves that belongs to the  $LS$  symmetry of  ${}^2D^e$ . For the  $\frac{3}{2}^+$  partial cross section, a small peak exists just above the first peak but no counterpart appears in the  $\frac{5}{2}^+$  partial cross section. This small peak at 243.26 eV may be assigned to the  $1s2p^2 {}^2P$  resonance [11]. Since the incident channels are  $1s^2\epsilon d^2 D_{3/2}$ , the  $1s2p^2 {}^2P_{3/2}$  resonance state can be formed only by the spin-orbit interaction. Therefore its overlap with the incident continuum is very small. The  $1s2p^2 {}^2P_{1/2}$  resonance state is also expected to appear in the  $\frac{1}{2}^+$  partial wave but its overlap with the  $1s^2\epsilon s^2 S_{1/2}$  may be too small to be scanned out in the calculation.

The partial cross sections for the  $1s2p^1 Pnl (n=4-16)$  resonances are shown in Fig. 3 that have been calculated by using the RMCT combining with the BS theory. The periodical feature with respect to the effective quantum number is observed. Two resonances of  $1s2p^1 Pnl {}^2L_J$  and  $1s2p^1 Pn(l+2) {}^2L_J$  appear in each period corresponding to an incident channel of  $1s^2\epsilon l^2 L_J (L=l)$ . The  $J^{\pi} = \frac{1}{2}^+$  partial wave is exceptional since only the  $1s2p^1 Pnp {}^2S_{1/2}$  resonance is possible for the incident channel of  $1s^2\epsilon s^2 S_{1/2}$ . The amplitude of the resonances decreases drastically above  $n=7$  resonance because then the  $1s2s^1 S\epsilon l$  and  $1s2p^3 P\epsilon l$  channels become open. The large overlap between the  $1s2p^1 Pnl (n \geq 8)$  resonance states and the  $1s2s^1 S\epsilon l$  continuum leads to an intensive Auger decay of those resonance states, which causes the sudden decrease of the DR probability. Contrasting to the  $1s2s^1 S\epsilon l$  channel, the  $1s2s^3 S\epsilon l$  continuum opening between the states of  $n=4$  and 5 at 298.978 eV affects the DR probability to some extent, but much less than the  $1s2s^1 S\epsilon l$  continuum does. That indicates a small overlap between the  $1s2p^1 Pnl$  resonances and the  $1s2s^3 S\epsilon l$  continuum.

Figure 4 gives the convolved partial cross section corresponding to Fig. 3 with the same temperature pairs as in Fig. 2. For the  $\frac{1}{2}^+$ ,  $\frac{3}{2}^+$ , and  $\frac{5}{2}^+$  partial waves, no sudden decrease appears between  $n=4$  and 5 resonances but a considerable reduction is observed for other partial waves. These can be explained by the decrease of the Auger rate with respect to the orbital momentum  $l$ . The  $1s2p^1 Pnp$  resonances are the main contributors for the  $\frac{1}{2}^+$ ,  $\frac{3}{2}^+$ , and  $\frac{5}{2}^+$  partial waves.

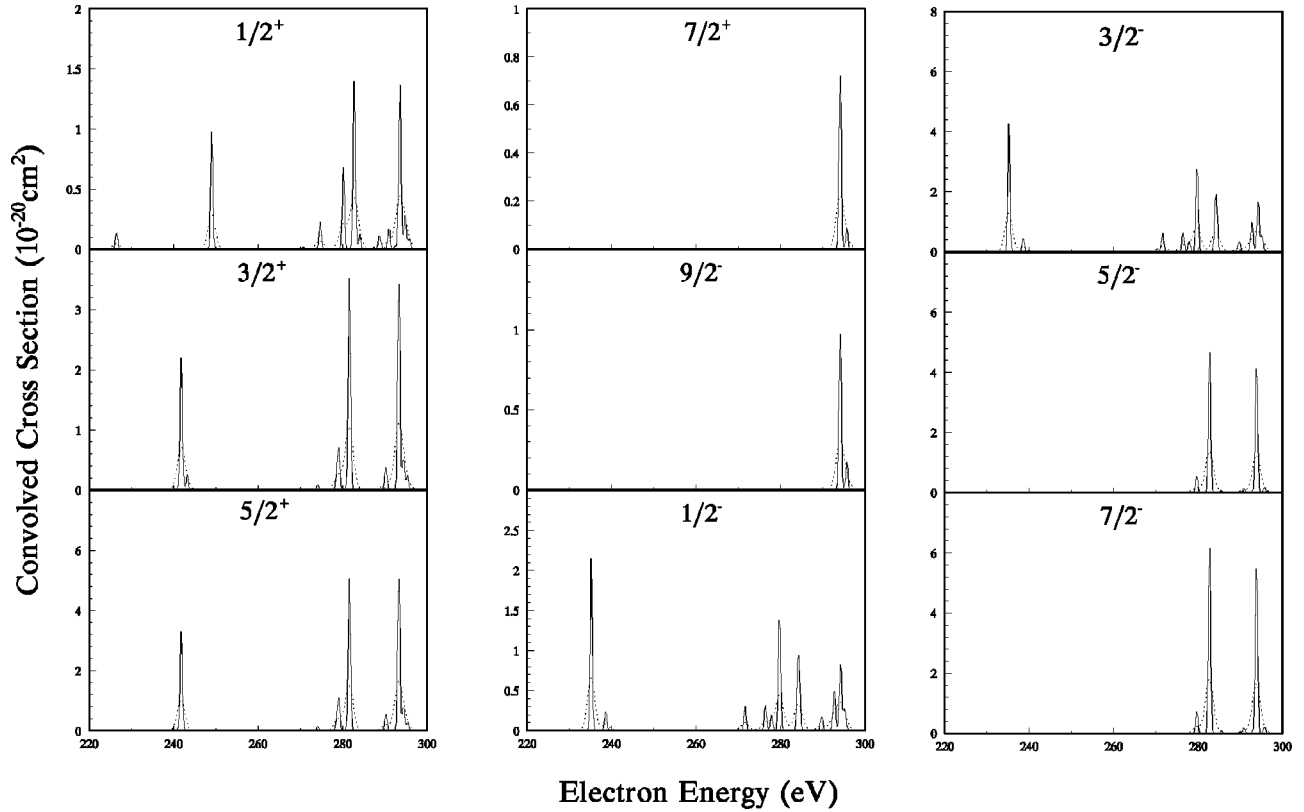


FIG. 2. Convolved partial cross sections for the  $n \leq 4$  resonance states vary with respect to the electron energy. The vertical temperatures  $T_{\perp}$  and longitudinal temperature  $T_{\parallel}$  are 80(120) meV and 0.11(1.5) meV for the solid (dotted) lines, respectively.

These resonances have a large Auger decay rate with respect to the  $1s^2\epsilon l$  channels. Therefore, the opening of the  $1s2s^3S\epsilon l$  channels has less influence on the DR cross sections. For the  $1s2p^1Pnl'$  ( $l' \geq 2$ ) resonances, the Auger decay rates to the  $1s^2\epsilon l$  channels decrease and become comparable with those of the  $1s2s^3S\epsilon l$  channels. These channels affect the DR cross sections considerably. The  $1s2p^1Pns$  resonances appear in the  $\frac{1}{2}^-$  and  $\frac{3}{2}^-$  partial waves just below the main resonances of  $1s2p^1Pnd$ . By comparing the  $n=4$  and 5 resonances, no sudden reduction appears for the  $1s2p^1Pns$  resonances series but it does for the main series of  $1s2p^1Pnd$  although the two series are not resolved completely for  $n=5$ . The  $\frac{11}{2}^+$ ,  $\frac{9}{2}^-$ , and  $\frac{11}{2}^-$  partial waves are from the  $1s2p^1Pnh$  and  $1s2p^1Png$  resonances. Therefore, the resonances start from  $n=5$  and 6, respectively.

The total cross section convolved with  $T_{\perp} = 120$  meV and  $T_{\parallel} = 1.5$  meV are shown in Fig. 5. The temperatures are obtained by fitting to the experimental spectrum of Kilgus *et al.* [11]. The solid line and the dashed line are from the RMCT and RMCT-BS methods, respectively. Both methods are applied to the  $n=4$  resonances to compare with each other. The result of RMCT is about 16% higher than that of RMCT-BS. Since the top part of the peak is very narrow, the difference between the integral cross sections should be small.

In Figs. 6–8, the present total DR cross sections for the  $n=2$ ,  $n=3-4$  and  $n=4-16$  resonances respectively are compared with the experimental measurement with a high

resolution [12]. Uniform RR backgrounds of 0.4, 0.3 and  $0.1 \times 10^{-20} \text{cm}^2$  are added to the calculated results for Figs. 6–8, respectively. For the resonances of  $1s2l2l'$  shown in Fig. 6, the calculated cross section is in good agreement with that of the observation. The resonance positions are about 0.5 eV lower than those of the measurement except for the  $1s2p^2^2S$  resonance that is about 1 eV higher. The first resonance of  $1s2s^2^2S_{1/2}$  at about 227 eV that has no radiative dipole decay channel completes a radiative decay through mixing with  $1s2p^2^2S_{1/2}$ . The small peak at 243.3 eV may assigned as the  $1s2p^2^2P$  resonance in *LS* couplings mentioned above. Inspecting the experimental spectrum carefully, one may find a dim peak at about 243.4 eV.

Figure 7 shows the cross section for the resonances of  $1s2lnl'$  ( $n=3,4$ ). The present results are in excellent agreement with those of the experiment for both the positions and the intensities of the resonances. The only exception is the shoulder at about 278.5 eV in the experimental spectrum that is reproduced in the present calculation. This shoulder may be from some very narrow resonances. They are missed in the calculation because widths of the resonances are smaller than the basic scan step.

The RMCT-BS method described in the theoretical part is adopted for the Rydberg resonances with the  $n \geq 4$  and only the radiative decay of the ionic core, namely  $1s2p^1P_1-1s^2^1S_0$  is considered here. It is found that the contributions from the partial wave with total angular momentum  $J$  larger than  $11/2$  are negligible, so the convergence of partial waves is well ensured. For  $n=4$ , as shown in Figs.

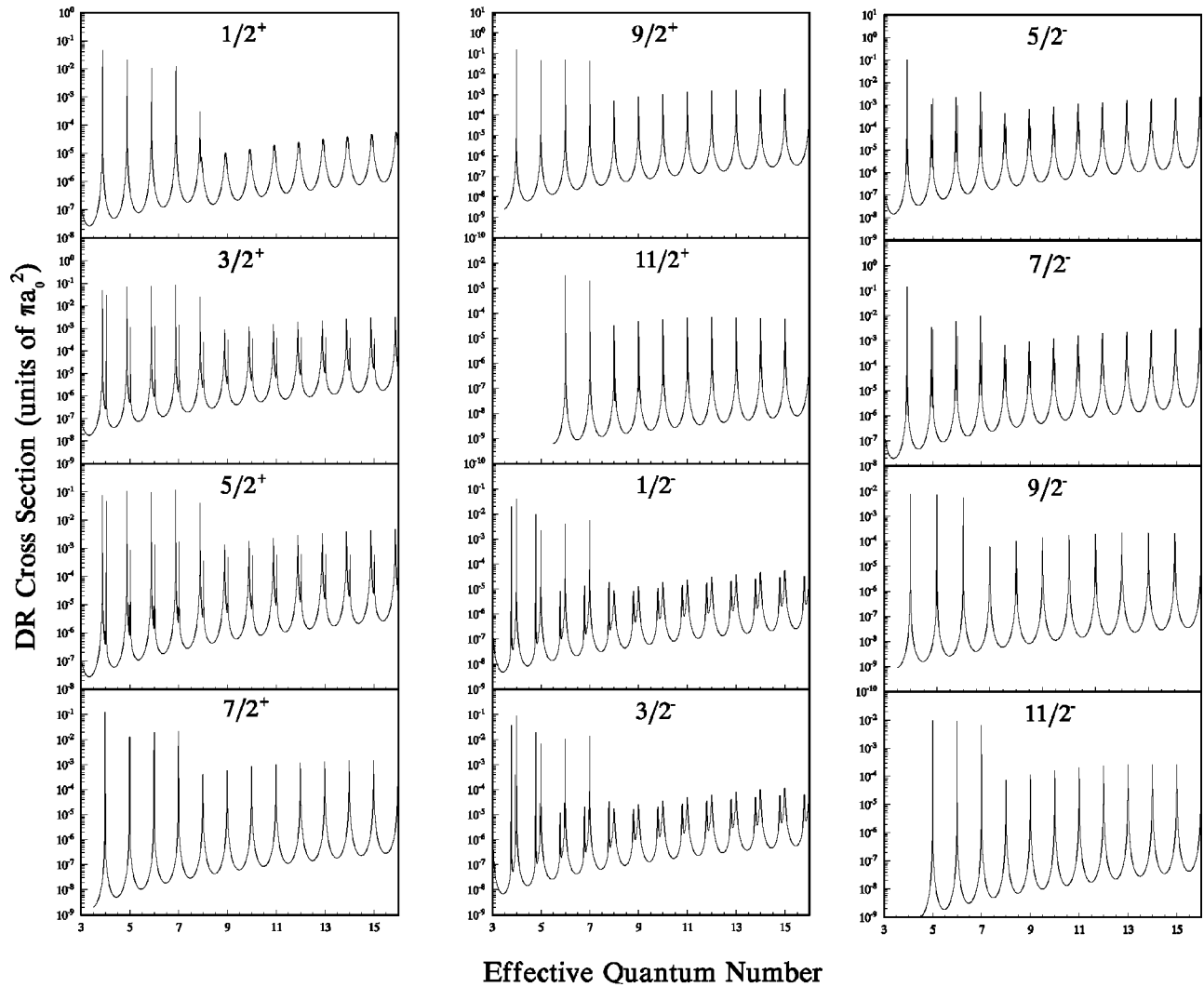


FIG. 3. Similar to Fig. 1 but for the  $1s2p\ ^1Pn_l$  ( $n=4-16$ ) resonances calculated with the RMCT-BS method.

7 and 8, both methods reproduce the experimental cross section, which suggests the second one is valid from  $n=4$ . The situation in the  $n \geq 5$  energy regime is more complicated than that in the  $n < 5$  regime since more Auger channels are open as mentioned above. The ionization thresholds are 298.978 eV for  $1s2s\ ^3S$ , 304.404 eV for  $1s2s\ ^1S$ , and 304.420 eV for  $1s2p\ ^3P$  [23]. For  $n=6$  and 7, the calculated peaks are substantially higher than those of the observation. The overestimation is consistent with the theoretical results of Kilgus *et al.* [11] and Pradhan *et al.* [8]. This discrepancy may be attributed to the couplings between the closed channels of  $1s2s\ ^1Sn_l$ ,  $1s2p\ ^3Pn'l'$ , and  $1s2p\ ^1Pn''l''$  that are not taken into account in the RMCT-BS method. Another possible cause for the discrepancy is the field ionization. Some loosely bounded resonance states may not survive the field ionization [12] in the experiment but are included in the calculation. The quantitative explanation needs further study.

According to Ref. [12], the Rydberg series are cut off at  $n_{\max}=16$  according to semiclassical estimation. However, as shown by the solid line in Fig. 8, the calculated peak corre-

sponding to  $n=9$  to 16 is narrower than that of the observation by about 1 eV. This discrepancy may be attributed to the radiative decay during the time of flight. The ions in a state with  $n > 16$  formed in DR can decay radiatively to the states with  $n \leq 16$  during the time of flight from the cooler to the analyzer. Therefore, they can survive field ionization and be counted in the experiment. With a larger value of  $n_{\max}$ , say 25, the discrepancy just disappears, as shown in Fig. 8 by the dotted line.

In summary, we have calculated the DR cross section due to  $\Delta N=1$  transitions for the ground state of  $C^{4+}$  with the relativistic multichannel theory combined with BS theory. The agreement with the observation is excellent in the whole regime except for  $n=6$  and 7 where the overestimation is probably due to the neglect of field ionization or the couplings of the closed channels. According to the present calculation, the Rydberg cutoff due to field ionization could be about  $n_{\max}=25$  to take into account the effect of the radiative decay during the time of flight. From the agreement with experiment, it would appear that the present method is applicable to both the low- $n$  and high- $n$  resonances.

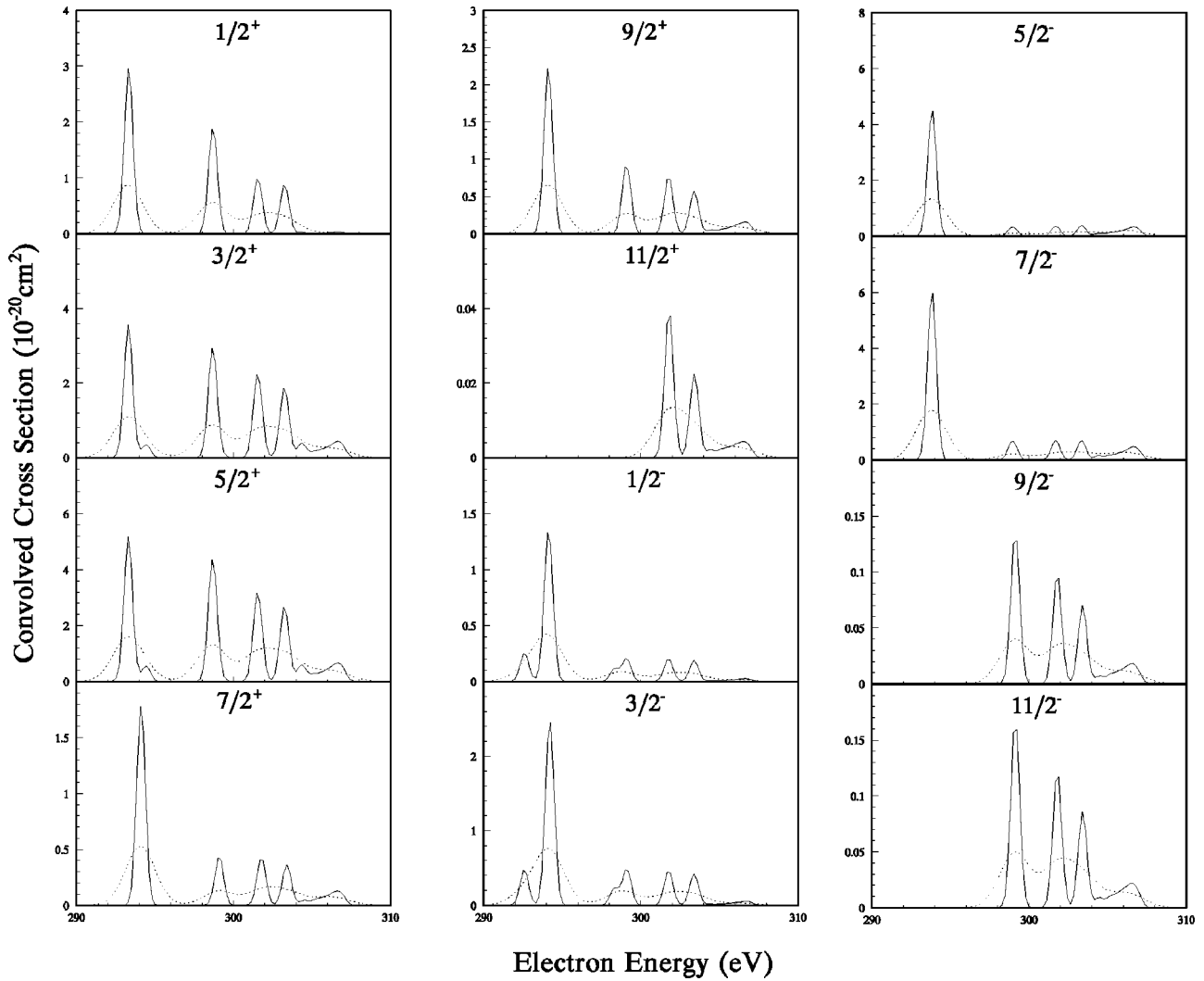


FIG. 4. Similar to Fig. 2 but for the  $1s2p^1Pnl(n=4-16)$  resonances calculated with the RMCT-BS method.

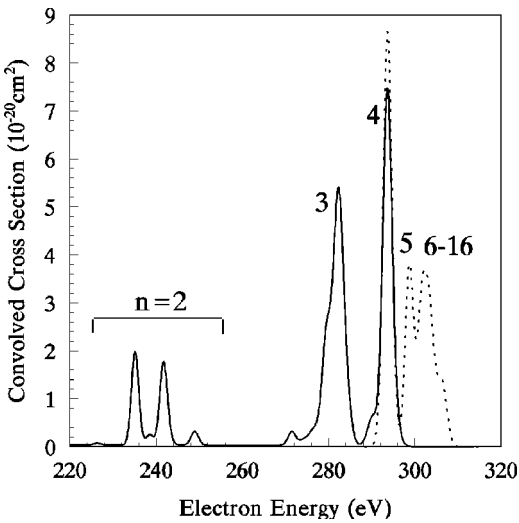


FIG. 5. Total cross sections convolved with  $T_{\perp}=120$  meV and  $T_{\parallel}=1.5$  meV. The solid line and the dashed line are from the RMCT and RMCT-BS methods, respectively.

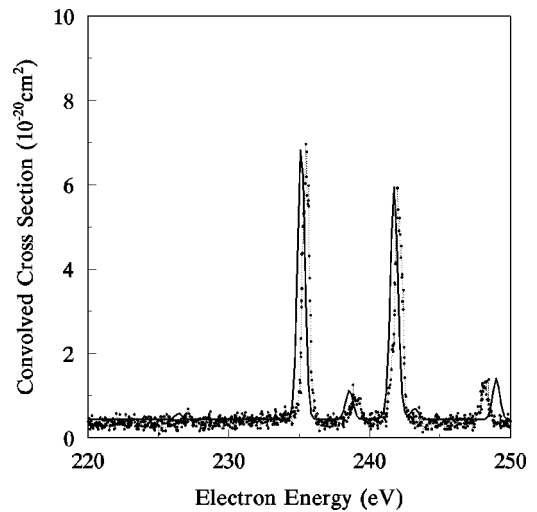


FIG. 6. Comparison of the calculated DR cross section with the experimental measurement for the  $1s2l2l'$  states of  $C^{3+}$ .

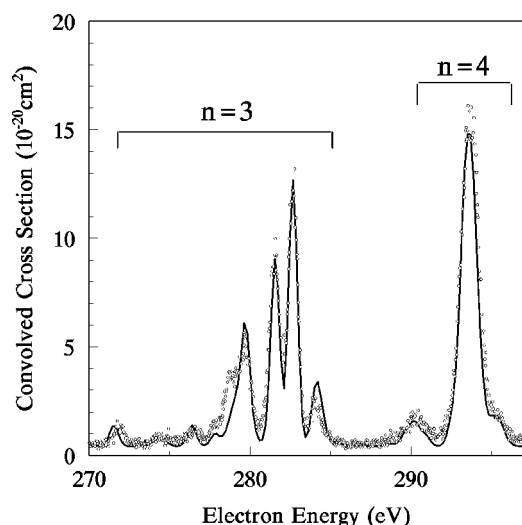


FIG. 7. Comparison of the calculated DR cross section with the experimental measurement for the  $1s2lnl'$  ( $n=3,4$ ) states of  $C^{3+}$ .

#### ACKNOWLEDGMENTS

The authors are grateful to Professor S. Mannervik for providing the experimental data in Figs. 6–8 and to Professor J. M. Li for invaluable advice. One of the authors (L.Y.)

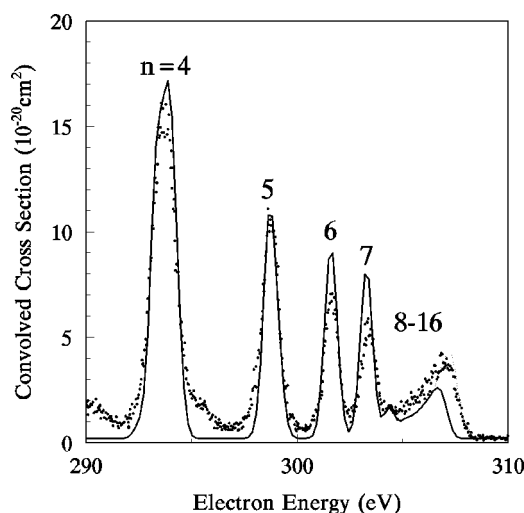


FIG. 8. Calculated and experimental DR cross sections for the  $1s2p^1P_1nl$  ( $n \geq 4$ ) states. The solid line and the dotted line corresponding to results which cutoff at  $n=16$  and  $n=25$ , respectively.

wishes to thank Dr. Wang Yi and Dr. Xu Ya-Qiong for their helpful discussions. This work is supported by the National Natural Science Foundation of China under Grant No. 19974006, and partially supported by the National High-Tech ICF Committee in China.

- 
- [1] A. Burgess, *Astrophys. J.* **139**, 776 (1964); **141**, 1588 (1965).
  - [2] M. J. Seaton and P. J. Storey, in *Atomic Processes and Applications*, edited by P. G. Burke and B. L. Moiseiwitsch (North-Holland, Amsterdam, 1976), p.133.
  - [3] J. Dubau and S. Volonte, *Rep. Prog. Phys.* **43**, 199 (1980).
  - [4] Y. Hahn, *Adv. At. Mol. Phys.* **21**, 123 (1985).
  - [5] L.H. Anderson, *Comments At. Mol. Phys.* **27**, 313 (1991).
  - [6] S. Mannervik *et al.*, *Phys. Rev. Lett.* **81**, 313 (1998).
  - [7] P.C.W. Davies and M.J. Seaton, *J. Phys. B* **2**, 757 (1969).
  - [8] A.K. Pradhan and H.L. Zhang, *J. Phys. B* **30**, L571 (1997).
  - [9] N.R. Badnell, T.W. Gorczyca, and A.D. Price, *J. Phys. B* **31**, L239 (1998).
  - [10] L.B. Zhao, A. Ichihara, and T. Shirai, *Phys. Rev. A* **62**, 022706 (2000).
  - [11] G. Kilgus, D. Habs, D. Schwalm, A. Wolf, R. Schuch, and N.R. Badnell, *Phys. Rev. A* **47**, 4859 (1993).
  - [12] S. Mannervik, S. Asp, L. Brostrom, D.R. DeWitt, J. Lidberg, R. Schuch, and K.T. Chung, *Phys. Rev. A* **55**, 1810 (1997).
  - [13] Y. Zou, L.B. Zhao, and Q.Y. Fang, *Phys. Rev. A* **60**, 4510 (1999).
  - [14] Yu Zou, Thesis, Institute of Physics, Chinese Academy of Science, 1994.
  - [15] Yu Zou, Xiao-Min Tong, and Jia-Ming Li, *Acta Phys. Sin.* **44**, 50 (1995).
  - [16] Wen Huang, Yu Zou, Xiao-Min Tong, and Jia-Ming Li, *Phys. Rev. A* **52**, 2770 (1995).
  - [17] D.R. DeWitt *et al.*, *Phys. Rev. A* **50**, 1257 (1994).
  - [18] D.R. DeWitt *et al.*, *J. Phys. B* **28**, L147 (1995).
  - [19] R.H. Bell and M.J. Seaton, *J. Phys. B* **18**, 1589 (1985).
  - [20] L.H. Andersen *et al.*, *Phys. Rev. Lett.* **62**, 2656 (1989).
  - [21] U. Fano, *Phys. Rev.* **126**, 1866 (1961).
  - [22] M.J. Seaton, *Rep. Prog. Phys.* **46**, 167 (1983).
  - [23] G.W. Drake, *Can. J. Phys.* **66**, 586 (1988).